

**THE DETERMINATION OF FRACTURE TOUGHNESS OF ROCKS  
BY CHEVRON-NOTCHED BRAZILIAN DISK SPECIMENS.**

by X. L. Zhao, J.-C. Roegiers, and M. Guo

School of Petroleum & Geological Engineering

The University of Oklahoma

Norman, Oklahoma 73019

**Abstract**

During the past decade, many laboratory techniques have been developed in an attempt to measure the fracture toughness of rocks. This has led, unfortunately, to a lack of consistency in the already scarce data bank. Differences as large as one order of magnitude have been reported for the same rock formation. In order to standardize the testing procedure, the International Society for Rock Mechanics recently published two Suggested Methods; one based on the Short Rod geometry (SR), and one on the bending of circular cores, the Chevron Edge Notch Round Bar in Bending test (CENRBB). However, these methods have some limitations; they will only provide Mode I fracturing parameters and are limited in scope as far as the propagation direction is concerned. Indeed, the SR can only accommodate crack propagation down the core length; while the CENRBB test imposes a fracture to propagate in a direction perpendicular to its axis. Hence, when considering for example the case of a man-induced hydraulic fracture, one of the pertinent horizontal growth directions cannot be studied by either test.

The Chevron-notched Brazilian Disk (CDISK) geometry, described in this paper, addresses this particular situation: it provides a complementary procedure allowing the investigation of lateral fracture propagation. Hence, the inherent toughness anisotropy can also be studied in great detail.

The advantages of this particular geometry can be summarized as follows: i) the specimen is core-based; ii) the measured fracture toughness is determined in the most pertinent direction, particularly when contemplating hydraulic fracturing stimulation treatments; iii) the specimen is easy to prepare; and, iv) the testing is trivial.

In addition to Mode I fracture tests, this approach may also be used to investigate mixed-mode fracturing situations.

Two types of rock were used in this preliminary study: a fine grained Vosges Sandstone and an Indiana Limestone. Different sizes of disks were also considered in order to investigate any potential size effect.

## Introduction

In recent years, more and more attention has been given to the application of fracture mechanics principles to geological engineering problems such as earthquake engineering (Li, 1987), rock cutting (Sanio, 1985; Zhao, 1989), rock blasting (Oucherylony, 1983; Fourney, 1983), and hydraulic fracturing (Roegiers et al., 1982; Cleary, 1983; Rummel, 1987; and Thiercelin, 1989). Recent developments in rock fracture mechanics were introduced in two series: Rock Fracture Mechanics edited by Rossmannith (1983); and Fracture Mechanics of Rocks edited by Atkinson (1987).

One of the most important rock fracture parameters, fracture toughness  $K_{Ic}$ , has been measured by several methods. The International Society for Rock Mechanics has recently proposed the Short Rod (SR) and Chevron Edge Notch Round Bar in Bending (CENRBB) geometries, shown in Figures 1 and 2, as suggested methods (ISRM, 1988). Those core-based specimens are particularly attractive for rock fracture toughness tests because they require a minimum of machining.

Those tests can provide the fracture toughness along several directions, but all coplanar, i.e., in a plane perpendicular to the core axis. However, in order to complete the investigation of any potential spatial rock anisotropy, an additional plug needs to be taken from the core, in a perpendicular direction. The direction of crack propagation in this third specimen will then most probably correspond to the direction of crack initiation when considering hydraulic fracturing situations at great depth.

Several test geometries have been proposed in the past, amongst them:

### Burst tests (internally notched) (BTI)

This corresponds to a pre-notched, internally pressurized, thick-walled cylinder, (but does not load the faces of the notch) (Figure 3) (Clifton et al., 1976 and Abou-Sayed et al., 1978). Although BTI is quite similar to hydraulic fracturing geometry, this technique has received little attention due to the experimental complexity.

### Semicircular bend tests (SCB)

Chong and Kuruppu (1984) developed this testing geometry, which has a single edge notch of length  $a$  and is loaded in a three-point bending configuration (Figure 4). SCB is especially suitable for applications requiring duplicate samples having similar composition, as such circular discs provide two duplicate specimens. Furthermore, the SCB can be used to study mixed-mode fracturing, by cutting a crack at an angle (Chong and Kuruppu, 1989).

### Radially cracked ring specimens (RCR)

This type of specimen has been used in measurements of strength of rock materials, and recently also in rock fracture tests by Thiercelin and Roegiers (1986), and Zhao (1989) (Figure 5).

Because of the geometry of the specimen and the uncertainty associated with the exact load transfer areas, theoretical determination of the exact stress intensity is difficult; hence, one needs also to rely on a complementary numerical technique (Zhao, 1989). If the internal radius of the ring is far smaller than the external radius, the ring specimen may be treated approximately as a cracked Brazilian disk (Thiercelin and Roegiers, 1986).

### Brazilian disk specimens (DISK)

In general, the Brazilian disk specimens, as shown in Figure 6, are used when attempting mixed-mode fracture toughness measurements (Awaji and Sato, 1978; Yatomi et al., 1989), but are usually not used to investigate Mode I fracturing tests due to inherent specimen preparation difficulties and complex calibration requirements.

In this paper an additional test geometry, the Chevron-notched Brazilian disk (CDISK) specimen, is discussed (Figure 7).

## Theoretical Background

### Straight-through Cracked Brazilian Disk Specimen

The solutions giving the stress intensity factor for a straight-through crack in a Brazilian disk specimen have been studied by Yarema and Krestin (1966), Libatskii and Kovchik (1967), Awaji and Sato (1978), Atkinson et al. (1982), and Yatomi et al. (1989).

Atkinson et al. (1982) expressed the solution as follows:

$$K_I = \frac{P}{\sqrt{\pi RB}} \sqrt{\alpha} N_I \quad (1)$$

where

$B$  = thickness of the disc;

$R$  = radius of the disk;

$\alpha = a/R$ ;  $a$  is the half-length of the crack;

$N_I$  = a non-dimensional stress intensity factor, determined by:

$$N_I = \sum_{i=1}^n T_i \alpha^{2i-2} A_i(\theta) \quad (2)$$

where

$A_i(\theta)$  = angular constants; and,

$T_i$  = numerical factors.

Shetty et al. (1985) used the following cubic polynomial to fit the above expression:

$$N_I = 0.991 + 0.141\alpha + 0.863\alpha^2 + 0.886\alpha^3 \quad (3)$$

and reported differences of less than 0.1%.

Yatomi et al. (1989) derived a solution for the case of  $\alpha < 0.2$ :

$$K_I = \frac{P}{\sqrt{\pi RB}} \sqrt{\alpha} \quad (4)$$

Yarema and Krestin (1966) and Libatskii and Kovchik (1967) used different methods to analyze the problem and obtained essentially the same results:

$$K_I = \frac{P}{\sqrt{2RB}} \sqrt{\alpha} \left( 1 + \frac{3}{2}\alpha^2 + \frac{3}{4}\alpha^6 + \frac{3}{64}\alpha^8 \right) \quad (5)$$

In this study, this last formula is used as a basic solution for the Brazilian disk containing a straight-through crack.

### Chevron-notched Brazilian Disk Specimen

Generally, there are three ways to determine the dimensionless stress intensity coefficient  $Y^*$  for a Chevron notched specimen: (i) *experimental determination of  $Y^*$  based on a comparison with  $K_{Ic}$  values obtained by the standardized methods;* (ii) *semi-analytical approach based on the compliance and the stress intensity factor determined for specimens with straight cracks;* and (iii) *numerical analyses using three-dimensional finite element or three-dimensional boundary element techniques.* By using a simplified analysis method proposed by Munz et al. (1980), the dimensionless stress intensity coefficient  $Y^*$  may be obtained for CDISK specimens.

Indeed, for specimens with a chevron notch, let's assume that the crack extends from an initial length  $a_0$  under increasing load. At crack length  $a$ , the crack front length,  $b$ , is given by (refer to Figure 7 for parameters definition):

$$b = B \left\{ 1 + \frac{2R}{B} \left[ (\Re^2 - \alpha_1^2)^{1/2} - (\Re^2 - \alpha^2)^{1/2} \right] \right\} \quad (6)$$

where

$$\alpha = a/R;$$

$$\alpha_0 = a_0/R;$$

$$\alpha_1 = a_1/R;$$

$$\Re = R_s/R; \text{ and,}$$

$$R_s = \text{radius of the saw.}$$

Calling upon Fracture Mechanics principles, the available energy for crack extension of  $\Delta a$  is given by:

$$\Delta U = \frac{P^2}{2W} \frac{dC}{d\alpha} \Delta\alpha \quad (7)$$

where

$W = 2R$ , width of specimen; and,

$C$  = the compliance of the specimen, i.e., load point displacement per unit of applied load.

On the other hand, the energy required for crack extension,  $\Delta\bar{W}$ , is given by:

$$\Delta\bar{W} = G_{IC} b \Delta a = \frac{K_{Ic}^2}{E'} b \Delta a \quad (8)$$

where

$$E' = \begin{cases} E, & \text{in the plane stress case;} \\ E/1 - \nu^2 & \text{in the case of plane strain.} \end{cases}$$

$b$  = the crack front length;

$\nu$  = Poisson's ratio; and,

$G_{IC}$  = fracture energy.

At all time, during stable crack propagation,  $\Delta U = \Delta\bar{W}$ , hence

$$K_{Ic} = \frac{P}{B\sqrt{W}} \left( \frac{1}{2k} \frac{dC'}{d\alpha} \right)^{1/2} \quad (9)$$

where

$C' = E'BC$ , the dimensionless compliance; and,

$$k = 1 + 2R \left( (\Re^2 - \alpha_1^2)^{1/2} - (\Re^2 - \alpha^2)^{1/2} \right) / B.$$

For the Chevron-notched specimens, the fracture toughness,  $K_{Ic}$  can be determined knowing the maximum load  $P_{max}$ :

$$K_I = \frac{P_{max}}{B\sqrt{W}} Y_m^* \quad (10)$$

where

$Y_m^*$  = minimum stress intensity coefficient.

Thus, from Eq.(9), one has

$$Y^* = \left( \frac{1}{2k} \frac{dC'}{d\alpha} \right)^{1/2} \quad (11)$$

To a first approximation, Munz et al. (1980) assumed that  $dC'/d\alpha$  for the Chevron notch is identical to that for a straight-through crack, which leads to:

$$\frac{dC'}{d\alpha} = 2Y^2 \quad (12)$$

where

$Y$  = the stress intensity coefficient for a straight crack for the specific geometry.

The relation between the stress intensity coefficients for a straight crack and Chevron notched crack may then be expressed as:

$$Y^* = \frac{Y}{\sqrt{k}} \quad (13)$$

From the solutions given by Yarema and Krestin (1966) and Libatskii and Kovchik (1967), for the Chevron-notched Brazilian disk specimen, we have:

$$Y^* = \sqrt{\frac{\alpha}{k}} \left( 1 + \frac{3}{2}\alpha^2 + \frac{3}{4}\alpha^6 + \frac{3}{64}\alpha^8 \right) \quad (14)$$

### The Minimum Stress Intensity Coefficients, $Y_m^*$

In order to calculate fracture toughness,  $K_{Ic}$ , the minimum stress intensity coefficients,  $Y_m^*$  are determined from Equation (14). In this study, disks with diameters of 2.125 in., 3.125 in., and 4.125 in. were used, while the slits on the surfaces were cut using a 3 in. or a 4 in. diameter saw. The results of minimum stress intensity coefficients and related non-dimensional crack lengths,  $\alpha_m$ , for such specimens are listed in Table I.

For the specimens with diameters of 3.125 in. and 4.125 in. cut by 3 in. diameter saw, the non-dimensional crack lengths  $\alpha_m$  were equal to  $\alpha_1$  in most cases. This means that the fracture toughness calculated by Equation (10) is the same as that given by a straight-through cracked specimen. In other words, the chevron notch in this situation is similar to the case of a pre-cracked geometry, as Shetty et al. (1985) used in their ceramics fracture tests.

### **Experimental Procedure**

Two types of rocks were used in this preliminary investigation: a fine grained Vosges Sandstone and an Indiana Limestone.

Specimens tested in this investigation consisted of 36 specimens of different sizes. Disks with diameters of 2.125 in., 3.125 in., and 4.125 in. were cut from the

rock blocks with a thickness of about 0.6 in., 0.6 in. and 1.0 in. A three inch wheel was used to introduce kerfs on the disk surfaces with less than 0.01 in. width. The specimens were dried at 110° for 5 hours and then air cooled before the tests, in order to minimize the possible effects of moisture content.

The tests were carried out using an MTS-Model 215 testing frame. The machine platen was moved at a rate of 0.04 in/min up to the maximum load. The load and load-point displacement were recorded by a Kipp & Zonen X-Y-Y(T) plotter and a PC computer.

## Results

Figure 8 shows a typical load vs. load-point displacement curve. The load was cycled several times before reaching the peak value. Each loading-unloading cycle may reveal a permanent deformation indicating that the crack has already propagated from the tip of Chevron-notch. In addition, the hysteresis changes with increasing load, a phenomenon which may be due to the process zone.

Table II summarizes all the test results obtained. To assess the effects of specimens' sizes, three different size of specimens were used. The differences found in the results given by the specimens with diameters of 3.125 in. and 4.125 in. are 21% for sandstone and 8% for limestone. The specimens with 2.125 in. diameters provided the highest values of fracture toughness: for sandstone, it is 37% higher than the value given by specimens with 3.125 in. diameter and 24% higher than that given by specimens with 4.125 in. diameter; and for limestone it is 13% and 20%, respectively.

## Discussion

The CDISK specimens used in this study have the following advantages: i) the specimens are core-based; ii) the measured fracture toughness is determined in the most pertinent direction, particularly when contemplating hydraulic fracturing stimulation treatments; iii) the specimens are easy to prepare; and, iv) the testing is easy to perform.

In addition to the above advantages, one of the outstanding features of CDISK is the existence of a compressive stress state near the tip of the crack, preventing the



development of a large process zone. More important, since this zone remains compressive throughout the fracture propagation phase, it prevents the process zone from reaching the sample end, affecting the load-carrying capacity of the specimen. Thus the fracture toughness may be determined directly from the maximum load.

The process zone at the crack tip indeed plays an important role in measuring fracture parameters via different specimen configurations. This influence may be quantified by comparing test results of rock samples containing different types of pre-cracks. Zhao (1984) carried out a series of 3-point bending beam tests using (i) a notch, (ii) a fatigue pre-crack, or (iii) a post-failure crack. He found that the measured apparent fracture toughness  $K_Q$  via a fatigue pre-cracked specimen is higher than the value obtained using a notched specimen, and is lower than the value determined with a post-failure crack. However, a very interesting phenomenon was observed (Figure 9). For the cases of notched or fatigue pre-cracked specimens, any unloading before reaching the peak load is linear elastic. On the contrary, for the case of post-failure cracked specimens, an hysteresis prevailed. One possible reason for this discrepancy is that there exists a larger fracture process zone near the tip of a post-failure crack; the associated stress field opposing opening of the crack during loading and favoring to their closing during unloading.

Considering the effects of a process zone, Barker (1979) proposed a plasticity correction factor to be introduced when computing the fracture toughness. The testing results have shown that when such a correction is applied,  $K_{Ic}^p$  values are approximately 25% to 50% above the so-called *apparent fracture toughness*  $K_Q$ . As the size of the process zone in rock fracture toughness testing is dependent on the grain size distribution, the loading conditions as well as the loading rate of the rock specimen, introduction of the plasticity correction may solve the problem to some degree. However, the most effective way to deal with the problem is to find a suitable geometry which limits the size of the process zone. The proposed CDISK fulfills this requirement.

## Summary

Chevron-notched Brazilian disk (CDISK) specimens are suitable for fracture toughness testing of rocks. The data generated by CDISK are the most relevant for hydraulic fracturing design considerations, as it usually coincides with the crack direction.

Based on a simplified method given by Munz et al. (1980), the minimum dimensionless stress intensity coefficient  $Y_m^*$  may be determined by:

$$Y^* = \sqrt{\frac{\alpha}{k}} \left( 1 + \frac{3}{2}\alpha^2 + \frac{3}{4}\alpha^6 + \frac{3}{64}\alpha^8 \right)$$

in which,

$$k = 1 + \frac{2R}{B} \left( (\mathfrak{R}^2 - \alpha_1^2)^{1/2} - (\mathfrak{R}^2 - \alpha^2)^{1/2} \right)$$

and the fracture toughness is then given by:

$$K_{Ic} = \frac{P}{B\sqrt{2R}} Y_m^*$$

Two types of rocks, a Berea Sandstone and an Indiana Limestone, were used in this study. The effect of specimens' sizes was investigated and the results show the existence of a size effect with values of fracture toughness much higher in the case of 2.125 in. diameter specimens.

## ACKNOWLEDGMENT

The authors wish to thank Shell Development Co. and the Gas Research Institute for their financial support of this work.

## References

- Abou-Sayed, A.S., Brechtel, C.E. and Clifton R.J., 1978, In situ stress determination by hydrofracturing: a fracture mechanics approach: Journal of Geophysical Research, v. 83, p. 2851-2862.
- Atkinson, C., Smelser, R.E., and Sanchez, J., 1982, Combined mode fracture via cracked Brazilian disk test: International Journal of Fracture, v. 18, no. 4, p. 279-291.

- Awaji, M. and Sato, S., 1978, Combined mode fracture toughness measurement by the disk test: Journal of Engineering Materials and Technology, Transactions of the ASME, v. 100, p. 175-182.
- Barker, L.M., 1979, Theory for determining  $K_{Ic}$  from small, non-LEFM specimens, supported by experiments on Aluminum: International Journal of Fracture, v. 15, no. 6, p. 515-536.
- Chong, K.P. and Kuruppu, M.D., 1988, New specimens for mixed mode fracture investigations of geomaterials: Engineering Fracture Mechanics, v. 30, no. 5, p. 701-712.
- Cleary, M.P., 1983, Modelling and development of hydraulic fracturing technology, in Rossmanith, ed., Rock Fracture Mechanics: CISM Courses and Lectures No. 275, p. 383-476.
- Clifton, R.J., Simonson, E.R., Jones, A.H. and Green, S.J., 1976, Determination of the critical stress intensity factor  $K_{Ic}$  from internally pressurized thick-walled vessels: Experimental Mechanics, June, p. 223-238.
- Fourney, W.L., 1983, Fracture control blasting; Fragmentation studies with small flaws; Fragmentation studies with large flaws, in Rossmanith, ed., Rock Fracture Mechanics: CISM Courses and Lectures No. 275, p. 301-352.
- ISRM, 1988, Suggested methods for determining the fracture toughness of rock: International Journal of Rock Mechanics and Mining Sciences & Geomechanics Abstracts, v. 25, no. 2, p. 72-96.
- Li, V.C., 1987, Mechanics of shear rupture applied to earthquake zones, in B.K. Atkinson, ed., Fracture Mechanics of Rocks. p. 351-428.
- Libarskii, L.L. and Kovchik, S.E., 1967, Fracture of discs containing cracks: Soviet Materials Science, no. 3, p. 334-339.
- Munz, D., Bubsey, R.T., and Srawley, J.E., 1980, Compliance and stress intensity coefficients for short bar specimens with chevron notches: International Journal of Fracture, v. 16, no. 4, p. 359-374.

- Ouchterlony, F., 1983, Analysis of cracks related to rock fragmentation, in Rossmannith, ed., Rock Fracture Mechanics: CISM Courses and Lectures No. 275, p. 31-68.
- Roegiers, J.-C., McLennan, J.D., and Schultz, L.D., 1982, In-situ stress determinations in northeastern Ohio: in 23rd Symposium in Rock Mechanics, University of California, Berkeley, p. 219-229.
- Rummel, F., 1981, Fracture mechanics approach to hydraulic fracturing stress measurements, in B.K. Atkinson, ed. Fracture Mechanics of Rocks: p. 217-240.
- Sanio H.P., 1985, Prediction of the performance of disc cutters in anisotropic rock: International Journal of Rock Mechanics and Mining Sciences & Geomechanics Abstracts, v. 22, no. 3, p. 153-161.
- Shetty, D.K., Rosenfield, A., and Duckworth, W.H., 1985, Fracture toughness of ceramics measured by Chevron-notch diametral compression test: Journal of American Ceramic Society, v. 68, no. 12, p. C325-C327.
- Thiercelin, M., 1989, Fracture toughness and hydraulic fracturing: International Journal of Rock Mechanics and Mining Sciences & Geomechanics Abstracts, v. 26, no. 3/4, p. 177-183.
- Yarema, S.Y. and Krestin, G.S., 1966, Determination of the modulus of cohesion of brittle materials by compressive tests on disc specimens containing cracks: Soviet Materials Science, v. 2, p. 7-10.
- Yatomi, C., Fujii, K., and Nakagawa, K., 1989, Combined stress hypothesis for mixed-mode fracture toughness criterion: Engineering Fracture Mechanics, v. 32, no. 6, p. 881-888.
- Zhao, X.L., 1984, An investigation on the methods of measuring rock fracture toughness: Fracture and Stress of Rock and Concrete. no. 1, p. 18-25 (in Chinese).
- Zhao, X.L., 1989, A fracture mechanics study of unassisted and water jet assisted rock disc cutting: Ph.D. Thesis, Department of Civil Engineering, University of Newcastle upon Tyne, 305 p.

Table I. The minimum stress intensity coefficients

$D_s$ in	$D$ in	$B$ in	$\alpha_1$	$a_1$ in	$a_0$ in	$a_m$ in	$Y_m^*$
3.0	2.125	0.6	1.00	1.063	0.635	0.896	2.992
			0.95	1.009	0.513	0.801	2.524
			0.90	0.956	0.362	0.689	2.120
			0.85	0.903	0.082	0.517	1.742
3.0	3.125	0.6	0.90	1.406	1.254	1.406	2.498
			0.85	1.328	1.120	1.328	2.193
			0.80	1.250	0.987	1.250	1.936
			0.75	1.172	0.850	1.172	1.717
			0.70	1.094	0.701	1.094	1.528
			0.65	1.016	0.528	1.016	1.364
			0.60	0.938	0.294	0.886	1.218
3.0	4.125	1.0	0.70	1.444	1.195	1.444	1.528
			0.65	1.341	0.935	1.341	1.364
			0.60	1.238	0.659	1.238	1.221
			0.55	1.134	0.236	1.134	1.094
4.0	3.125	0.6	1.0	1.563	1.266	1.563	3.297
			0.95	1.484	1.144	1.484	2.862
			0.90	1.406	1.017	1.394	2.497
			0.85	1.328	0.881	1.283	2.186
			0.80	1.250	0.732	1.167	1.917
			0.75	1.172	0.558	1.037	1.679
			0.70	1.094	0.320	0.869	1.460
4.0	4.125	1.0	0.90	1.856	1.566	1.856	2.499
			0.85	1.753	1.364	1.753	2.194
			0.80	1.650	1.159	1.650	1.936
			0.75	1.547	0.936	1.547	1.716
			0.70	1.444	0.672	1.375	1.524
			0.65	1.341	0.254	1.091	1.332

$D_s$  = diameter of the saw

$D$  = diameter of the rock specimen

$B$  = thickness of the rock specimen

Table II. The test results

Specimen Identification	Diameter in	$a_0$ in	$a_m$ in	$a_1$ in	$P_{max}$ pound	$K_{Ic}$ psi $\sqrt{\text{in}}$	$K_{Ic}$ Mpa $\sqrt{\text{m}}$
SDA1	2.125	0.487	0.781	0.985	200.0	570.4	0.627
SDA2	2.125	0.512	0.799	0.990	182.5	541.5	0.595
SDA3	2.125	0.418	0.727	0.960	335.0	880.1	0.967
SDA4	2.125	0.480	0.775	0.980	275.0	780.4	0.858
Mean						693.1	0.762
LDA1	2.125	0.568	0.842	0.990	415.0	1379.8	1.516
LDA2	2.125	0.426	0.737	1.035	630.0	1509.7	1.659
LDA3	2.125	0.431	0.737	0.950	420.0	1143.5	1.257
LDA4	2.125	0.498	0.788	0.965	540.0	1622.3	1.783
Mean						1413.8	1.554
SDB1	3.125	0.400	0.950	0.950	372.5	459.3	0.505
SDB2	3.125	0.224	0.840	0.889	412.5	483.0	0.531
SDB3	3.125	0.427	0.935	0.935	385.0	499.8	0.549
SDB4	3.125	0.187	0.788	1.01	207.5	288.5	0.258
Mean						432.5	0.475
LDB1	3.125	0.224	0.809	1.025	950.0	1325.0	1.456
LDB2	3.125	0.087	0.747	1.073	1040.0	1306.6	1.436
LDB3	3.125	0.216	0.807	1.015	770.0	1080.7	1.188
LDB4	3.125	0.163	0.777	1.08	965.0	1232.2	1.354
Mean						1236.1	1.359
SDC1	4.125	0.111	1.038	1.315	785.0	508.7	0.559
SDC2	4.125	0.180	1.054	1.315	885.0	561.7	0.617
SDC3	4.125	0.702	1.405	1.450	700.0	534.9	0.588
SDC4	4.125	0.629	1.341	1.420	640.0	477.0	0.524
SDC5	4.125	0.659	1.368	1.430	725.0	546.9	0.601
Mean						525.8	0.578
LDC1	4.125	0.565	1.296	1.415	1670.0	1196.1	1.314
LDC2	4.125	0.567	1.295	1.385	1440.0	1064.3	1.170
LDC3	4.125	0.5651	1.296	1.415	1640.0	1174.7	1.291
LDC4	4.125	0.516	1.255	1.375	1550.0	1118.4	1.229
Mean						1138.4	1.251

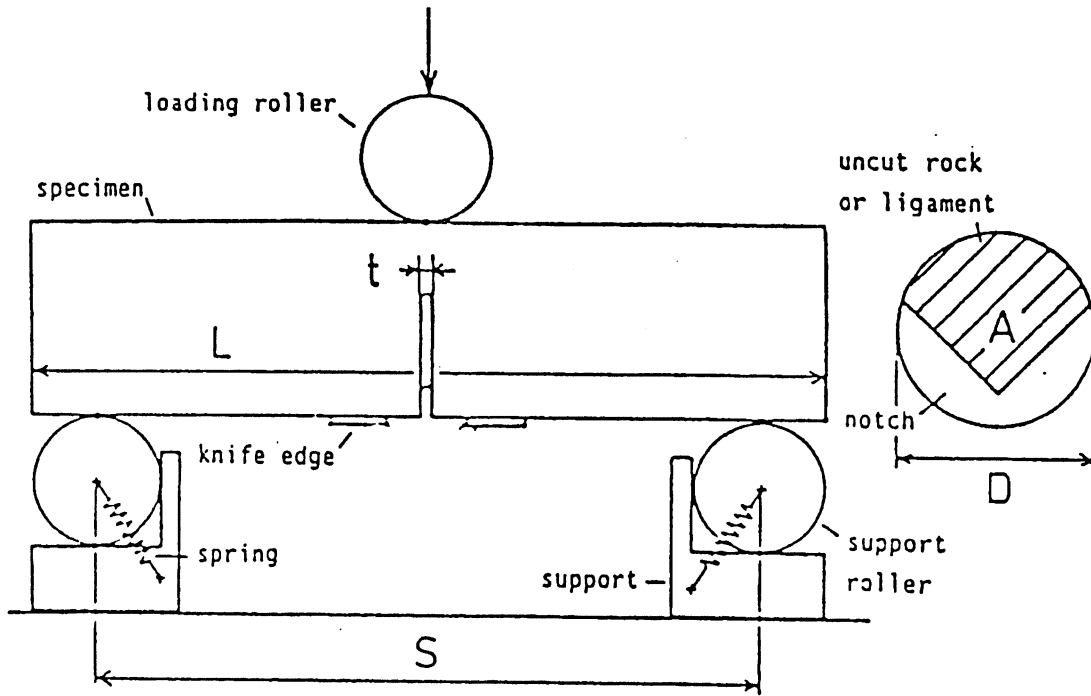


Figure 1. Chevron bend specimen

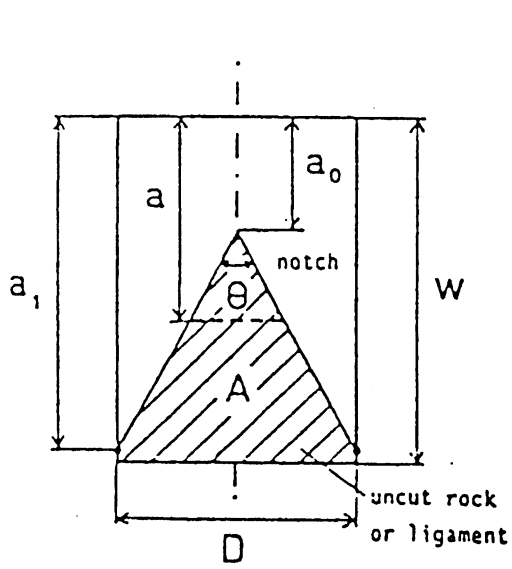


Figure 2. Short rod specimen

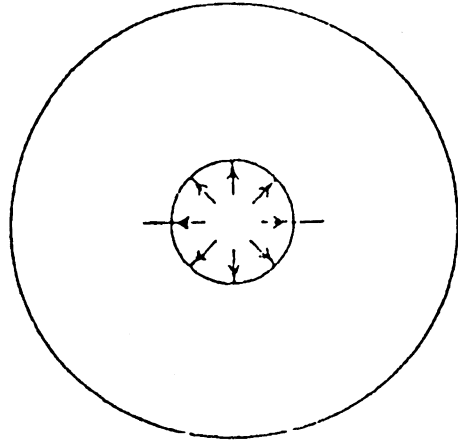


Figure 3. Burst tests

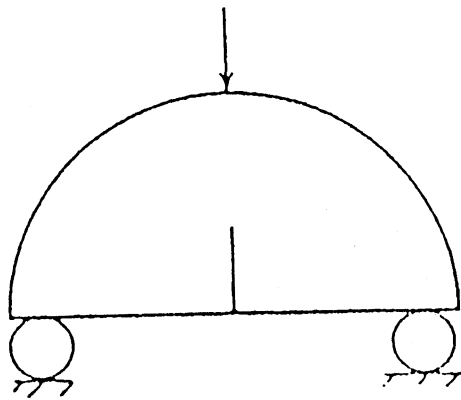


Figure 4. Semi-circular bend specimen



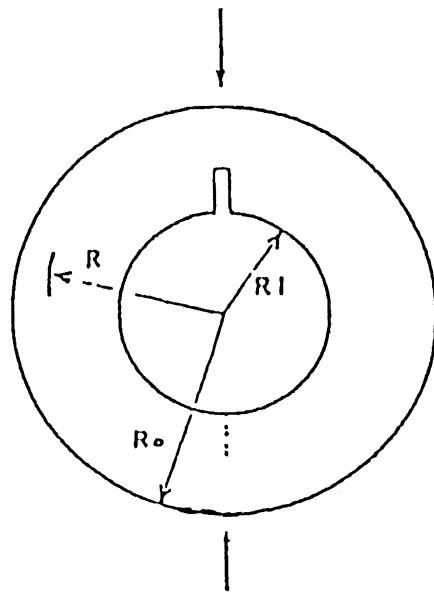


Figure 5. Radially cracked ring specimen

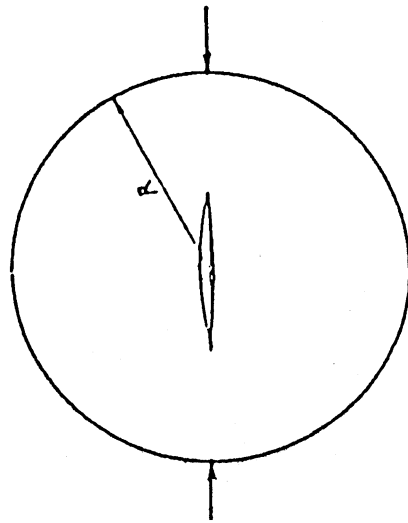


Figure 6. Brazilian disk specimen

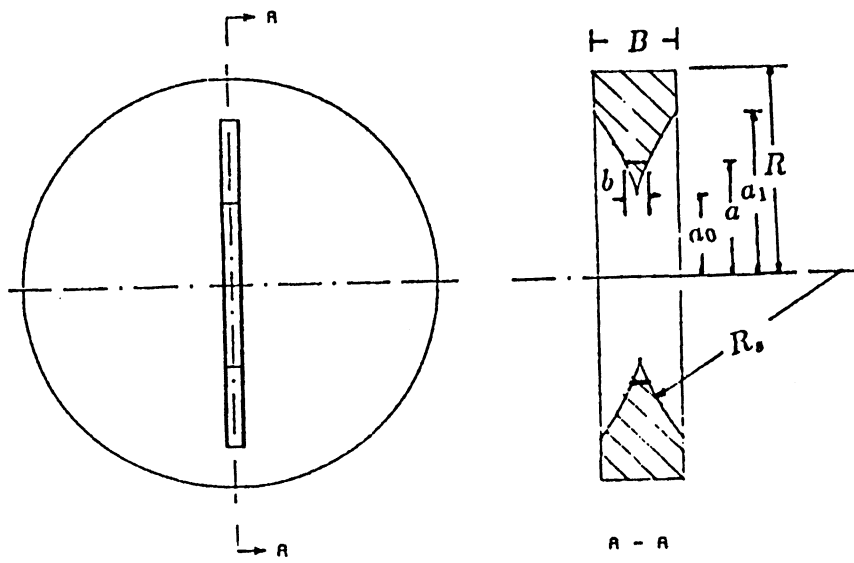


Figure 7. Chevron-notched Brazilian disk (CDISK) specimen

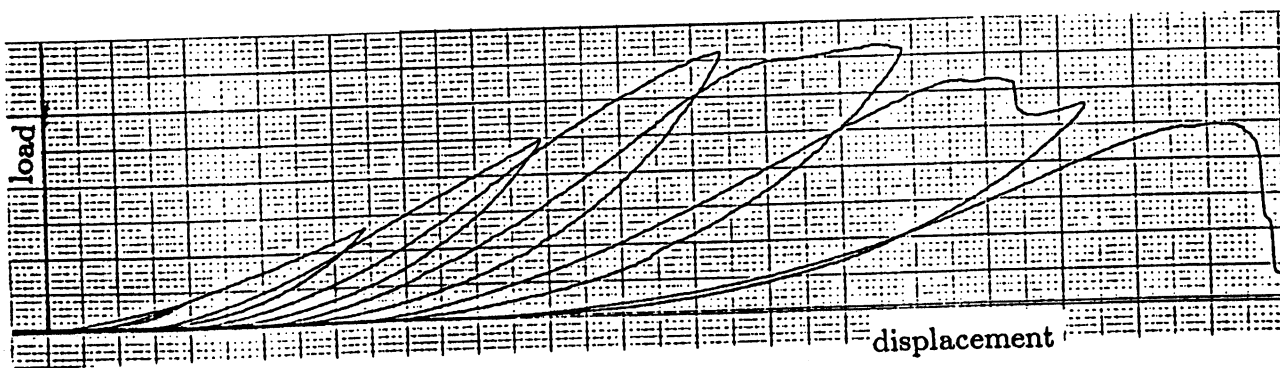
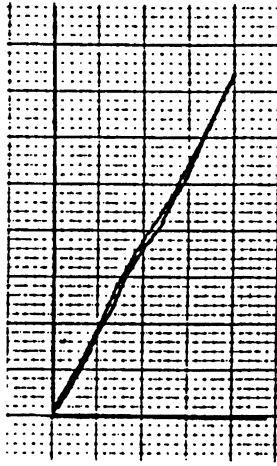
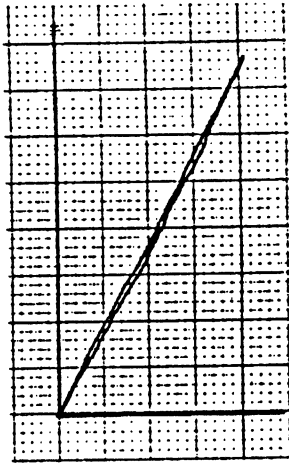


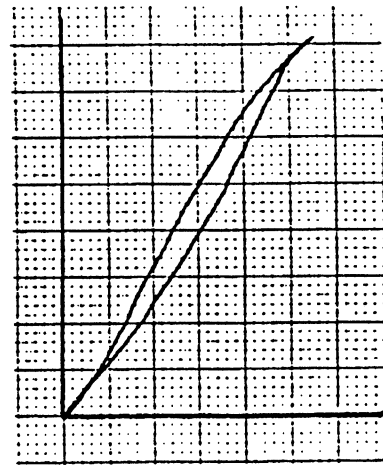
Figure 8. Typical load vs. load-point displacement



(a) notched crack



(b) fatigue pre-crack



(c) post-failure crack

Figure 9. Loading-unloading paths for specimens with different pre-cracks

